

## Two-Dimensional Assembly of Rod Amphiphiles into Planar Networks

Jung-Keun Kim,<sup>†</sup> Eunji Lee,<sup>†</sup> Young-Hwan Jeong,<sup>†</sup> Jeong-Kyu Lee,<sup>‡</sup> Wang-Cheol Zin,<sup>‡</sup> and Myongsoo Lee<sup>\*†</sup>

Center for Supramolecular Nano-Assembly and Department of Chemistry, Yonsei University, Seoul 120-749, Korea, and Department of Materials Science and Engineering, Polymer Research Institute, Pohang University of Science and Technology, Pohang 790-784, Korea

Received February 27, 2007; E-mail: mslee@yonsei.ac.kr

The ability of rod building blocks to self-assemble into supramolecular structures provides unique opportunities for the design of nanoscale materials with predictable properties and functions.<sup>1</sup> Extensive efforts thus have been directed toward supramolecular systems for exploration of novel properties and functions that are not easily available without specific assembly of molecular components. Aggregation of rod building blocks in solution can generate various one-dimensional nano-objects including helices,<sup>2</sup> ribbons,<sup>3</sup> tubules,<sup>4</sup> and rings,<sup>5</sup> depending on the molecular structure. The hierarchical assembly of such one-dimensional structures could result in the formation of three-dimensional (3D) networks through interconnecting the extended micelles.<sup>6</sup> On the other hand, anisotropic interactions of nanoparticles result in the spontaneous formation of a free-suspended 2D structure in solution.<sup>7</sup> Similarly, surface-layer proteins in bacterial cells are well established to self-assemble into 2D structures with in-plane ordered arrays of pores through anisotropic interactions between the individual subunits.<sup>8</sup> However, self-assembly of synthetic molecules into planar nets remains unexplored.<sup>9</sup>

We present here the spontaneous formation of nanoporous sheets in aqueous solution without a template to guide them, which is based on the self-assembly of dumbbell-shaped rod amphiphiles driven by a fine balance of anisotropic hydrophobic interactions and steric constraints endowed with bulky dendritic wedges. The dumbbell-shaped rod amphiphiles that form these aggregates consist of a stiff rod segment that is grafted by hydrophilic polyether dendrons at one end and hydrophobic branches at the other end ( $f_{\text{alkyl/PEO}} = 0.97$ ) (Figure 1). Transmission electron microscopy (TEM) studies showed that both molecular dumbbells self-assemble into stable 2D aggregates. Figure 2a shows a low magnification micrograph obtained from the 0.01 wt % aqueous solution of **1** cast onto a TEM grid. The negatively stained sample with uranyl acetate shows a single layer of planar nets with protruding cylinders and closed loops against a dark background (Figure 2a). The image at higher magnification shows that the nets consist of interconnected cylindrical components with a uniform cross-section of 16 nm and in-plane ordered packing of pores with a diameter of  $\sim 15$  nm (Figure 2b). The Fourier transform shown as an inset to Figure 2b indicates that the pores are arranged into a roughly 2D hexagonal symmetry with a lattice dimension of  $\sim 30$  nm. For direct imaging of the 2D objects formed in aqueous solution, cryogenic TEM (cryo-TEM) experiments were performed with a 0.01 wt % aqueous solution.<sup>10</sup> A large area micrograph shows dark, wrinkled sheets against the vitrified solution background (Figure 2c), demonstrating that the 2D structure forms in bulk solution, not on the substrates during drying process. A zoomed-in image clearly shows that these

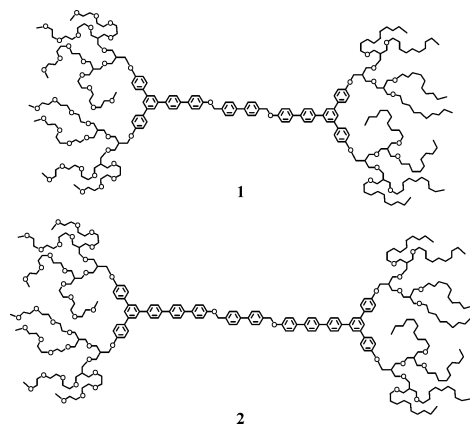


Figure 1. Chemical structure of rod amphiphiles **1** and **2**.

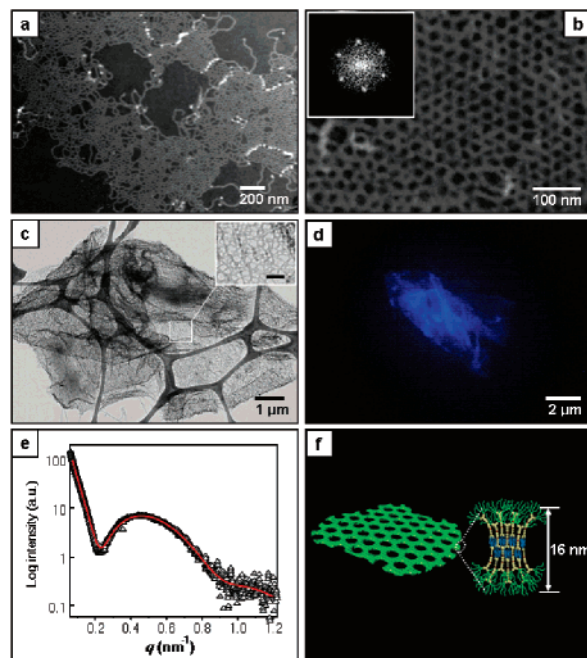


Figure 2. (a) The low-magnification and (b) high-magnification TEM images of sample cast from aqueous solution of **1**. (Inset) Fourier diffractogram of image. (c) Cryo-TEM image of aqueous solution of **1**. (Inset) Zoomed-in image, scale bar is 100 nm. (d) Fluorescence micrograph in aqueous solution of **1**. (e) The SAXS profile of **1** plotted against  $q$  ( $=4\pi \sin \theta/\lambda$ ). (f) Schematic representation of a network structure of **1** in aqueous solution (blue, hydrophobic branches; green, polyether dendrons).

sheets are based on a network structure with a uniform cylindrical cross-section.

The formation of the 2D objects in aqueous solution was further confirmed by fluorescence microscopy with the 0.01 wt % aqueous

<sup>†</sup> Yonsei University.

<sup>‡</sup> Pohang University of Science and Technology.

solution of **1** (Figure 2d). The image shows the formation of free-floating 2D objects that appear as flat, semifolded, and even wrinkled platelets, again demonstrating that the 2D objects form in solution rather than on the substrates. Small-angle X-ray scattering (SAXS) measurements were performed for determination of the thickness of the 2D objects formed in aqueous solution. The profile taken from a 5 wt % aqueous solution shows a strong scattering together with weak shoulder at a higher  $q$ -region (Figure 2e). This scattering profile can be best fitted using the form factor expression as an inhomogeneous lamellar model with a thickness of 16 nm.<sup>11</sup> Comparison with the estimated length of a fully extended molecular unit of about 8.4 nm suggests that the 16 nm thickness arises from a bilayer packing in which the hydrophobic alkyl chains are intercalated between the rod segments (Figure 2f).

In an attempt to understand the mechanism of 2D network formation, TEM experiments were performed at different stages of structural rearrangements (Supporting Information Figures S4 and S5). The image, at initial stages, shows the formation of spherical micelles with an average core diameter of 17 nm. An increase in time reveals the formation of branched cylinders and toroids with mostly 3-fold junctions at the expense of the short cylindrical and spherical micelles. A further increase in time reveals planar network fragments with diameters of lateral pores ranging from several tens to a few hundred nanometers. Eventually, these 2D fragments with large pores were observed to further assemble to form extended networks with decreased pores in diameter ranging from 15 to 30 nm which remain to be essentially unaltered over a period of 6 months. It is interesting to note that, with decreasing the pore size, the pores appear to be more regular in diameter. This observation leads us to speculate that the equilibrium 2D structure would be perforated sheets with in-plane hexagonally ordered pores. This is supported by the TEM micrograph taken from cast film of aqueous solution that shows a set of fairly uniform pores with a 2D hexagonal symmetry (Figure 2b).

The results described above represent that the self-assembled structure successively changes, from spheres, short cylinders, branched cylinders together with toroids to 2D networks. This evolution in the self-assembled structure with time can be rationalized by considering the strong tendency of rod blocks to form anisotropic arrangement and consequent space filling requirements.<sup>12</sup> The core of the discrete aggregates is composed of hydrophobic dendritic wedges and rod segments, which are encapsulated in a shell of the hydrophilic dendrons in contact with water. Considering an extreme steric problem of stiff rod segments to be radially packed, the more parallel arrangement of the rod segments is expected to be the best way to close-packing the hydrophobic core, as supported by TEM and SAXS. In this case, hydrophilic dendritic wedges are too short to stretch beyond the extended hydrophobic length. Accordingly, the aggregates may consist of hydrophilic caps and hydrophobic side face that create a huge energetic penalty for exposing the hydrophobic edges to the aqueous environment. To reduce the unfavorable contact between hydrophobic edges and water, the micelles would be held together through anisotropic interactions, giving rise to 2D nets passing through intermediate structures such as branched cylinders and toroids.

The formation of a planar network structure stimulated us to investigate if an increase in rod length drives the system toward a closed 2D structure through increasing rod-rod interactions. With

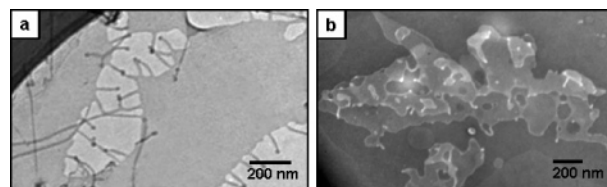


**Figure 3.** (a) Cryo-TEM image from aqueous solution of **2**; (b) TEM image (negatively stained with uranyl acetate) of sample cast from aqueous solution of **2**.

this consideration in mind, we have prepared **2** based on a longer rod. The aggregation behavior of **2** in dilute aqueous solutions was investigated by means of fluorescence microscopy and TEM. Similar to **1**, the fluorescence microscopy image of **2** (a 0.01 wt % aqueous solution) shows sheetlike aggregates as large as several micrometers.<sup>13</sup> However, cryo-TEM with the 0.01 wt % aqueous solution revealed closed 2D sheets with protruding short cylinders (Figure 3a). This result indicates that increasing rod length decreases interfacial curvature and thus can enforce perforated sheets to closed 2D structure. Therefore, the primary driving force responsible for the formation of the pores in the sheets seems to be the balance between the hydrophilic interaction of the polyether dendrons and the hydrophobic interaction of the rod and alkyl segments. Such a unique arrangement of rigid rod building blocks might provide a new strategy for the design of nanoporous materials simultaneously with biological and electro-optical functions.

**Acknowledgment.** This work was supported by the National Creative Research Initiative Program of the Korean Ministry of Science and Technology. E.L. thanks the Seoul Science Fellowship Program, and J.-K.K., E.L., Y.-H.J., and J.-K.L. acknowledge a fellowship of the BK21 program from the Ministry of Education and Human Resources Development.

**Supporting Information Available:** Synthetic and other experimental details. This material is available free of charge via the Internet at <http://pubs.acs.org>.

## References

- (1) (a) Lee, M.; Cho, B.-K.; Zin, W.-C. *Chem. Rev.* **2001**, *101*, 3869–3892. (b) Klok, H.-A.; Lecommandoux, S. *Adv. Mater.* **2001**, *13*, 1217–1229.
- (2) Hoeben, F. J. M.; Jonkheijm, P.; Meijer, E. W.; Schenning, A. P. H. J. *Chem. Rev.* **2005**, *105*, 1491–1546.
- (3) Zubarev, E. R.; Pralle, M. U.; Sone, E. D.; Stupp, S. I. *J. Am. Chem. Soc.* **2001**, *123*, 4105–4106.
- (4) (a) Hill, J. P.; Jin, W.; Kosaka, A.; Fukushima, T.; Ichihara, H.; Shimomura, T.; Ito, K.; Hashizume, T.; Ishii, N.; Aida, T. *Science* **2004**, *304*, 1481–1483. (b) Yang, W.-Y.; Lee, E.; Lee, M. *J. Am. Chem. Soc.* **2006**, *128*, 3484–3485.
- (5) Kim, J.-K.; Lee, E.; Huang, Z.; Lee, M. *J. Am. Chem. Soc.* **2006**, *128*, 14022–14023.
- (6) (a) Bernheim-Groswasser, A.; Tlustý, T.; Safran, S. A.; Talmon, Y. *Langmuir* **1999**, *15*, 5448–5453. (b) Jain, S.; Bates, F. S. *Science* **2003**, *300*, 460–464.
- (7) Tang, Z.; Zhang, Z.; Wang, Y.; Glotzer, S. C.; Kotov, N. A. *Science* **2006**, *314*, 274–278.
- (8) Sleytr, U. B.; Messner, P.; Pum, D.; Sára, M. *Angew. Chem., Int. Ed.* **1999**, *38*, 1034–1054.
- (9) Li, Z.; Hillmyer, M. A.; Lodge, T. P. *Nano Lett.* **2006**, *6*, 1245–1249.
- (10) (a) Edmonds, W. F.; Li, Z.; Hillmyer, M. A.; Lodge, T. P. *Macromolecules* **2006**, *39*, 4526–4530. (b) Li, Z.; Kesselman, E.; Talmon, Y.; Hillmyer, M. A.; Lodge, T. P. *Science* **2004**, *306*, 98–101.
- (11) Pedersen, J. S. *J. Appl. Crystallogr.* **2000**, *33*, 637–640.
- (12) Williams, D. R. M.; Fredrickson, G. H. *Macromolecules* **1992**, *25*, 3561–3568.
- (13) See Supporting Information.

JA071394Y